Available online at www.sciencedirect.com

SCIENCE DIRECT®

Journal of Organometallic Chemistry 691 (2006) 3336–3342

Journal of Organometallic Chemistry

www.elsevier.com/locate/jorganchem

Photochemical reactions of $Fe(CO)_5$ with FcC≡CH in the presence of S-powder and CS_2: Synthesis and characterization of $[\{\mu\text{-SC(H)=C(Fc)S}\}(CO)_6Fe_2]$, $[\mu\text{-SC(O)C(H)=C(Fc)S}\}(CO)_6Fe_2]$; *cis*-$[\mu\text{-}\eta^1{:}\eta^2{:}\eta^1{:}\eta^1\text{-}\{C(Fc)=C(H)CS_2C(H)=C(Fc)\}(CO)_6Fe_2]$ and *trans*-$[\mu\text{-}\eta^1{:}\eta^2{:}\eta^1{:}\eta^1\text{-}\{C(Fc)=C(H)CS_2C(Fc)=C(H)\}(CO)_6Fe_2]$

Pradeep Mathur [a,b,*], Vinay K. Singh [a], Amrendra K. Singh [a],
Shaikh M. Mobin [b], Carsten Thöne [c]

[a] *Chemistry Department, Indian Institute of Technology Bombay, Powai, Bombay 400 076, India*
[b] *National Single Crystal X-ray Diffraction Facility, Indian Institute of Technology Bombay, Powai, Bombay 400 076, India*
[c] *Institut für Anorganische Chemie, TU Braunschweig, Hagenring 30, Braunschweig 38106, Germany*

Received 11 April 2006; received in revised form 17 April 2006; accepted 17 April 2006
Available online 26 April 2006

Abstract

Photolysis of a hexane solution containing $Fe(CO)_5$, ferrocenylacetylene and S-powder under argon at −30 °C led to the formation of two different products: $[\{\mu\text{-SC(H)=C(Fc)S}\}(CO)_6Fe_2]$ (**1**) and $[\{\mu\text{-SC(O)C(H)=C(Fc)S}\}(CO)_6Fe_2]$ (**2**) featuring new C–S, C–C, Fe–Fe and Fe–S bond formations. In presence of CS_2, formation of *cis*-$[\mu\text{-}\eta^1{:}\eta^2{:}\eta^1{:}\eta^1\text{-}\{C(Fc)=C(H)CS_2C(H)=C(Fc)\}(CO)_6Fe_2]$ (**5**) and *trans*-$[\mu\text{-}\eta^1{:}\eta^2{:}\eta^1{:}\eta^1\text{-}\{C(Fc)=C(H)CS_2C(Fc)=C(H)\}(CO)_6Fe_2]$ (**6**) was observed, along with **1**. All new compounds were characterized by IR and ^1H and ^{13}C NMR spectroscopy. Structures of **1**, **2**, **5** and **6** were established crystallographically.

Keywords: Iron carbonyl clusters; Acetylene; Chalcogen; Crystal structures

1. Introduction

Activation of acetylene on transition metal complexes is of considerable importance, because the reduction of acetylene to olefins is an important probe of the active metallic center in the enzyme nitrogenase [1] and because there is interest in transforming the coordinated alkynes into useful organic species [2]. Although there exist a large number of reports on the different types of bonding modes of acetylenes to transition metals [3], investigations on activation of acetylenes on main group elements are more recent and far fewer. Several research groups have been working on the use of alkynes as bridging ligands in cluster formation, preparation of metal acetylides and subsequent investigation of acetylide coupling reactions on cluster frameworks [3d–6]. Recently, we reported on the photochemical reaction of ferrocenylacetylene with iron pentacarbonyl to form 2,5- and 2,6-diferrocenylquinone [7]. Formation of the quinones was shown to proceed via an intermediate, tetracarbonyl(2-ferrocenylmaleoyl)iron. With less bulky acetylenes, formation of substituted quinones was not observed. Contrast in behavior of ferrocenylacetylene and phenylacetylene has also been observed in their reactions with mixtures of $[Fe_3(CO)_9(\mu_3\text{-}S)_2]$ and $[(\eta^5C_5\text{-}Me_5)M(CO)_3(CCPh)]$ (M = Mo, W); when monometal acetylides, $[(\eta^5\text{-}C_5Me_5)M(CO)_3(CCPh)]$ (M = Mo, W),

---

[*] Corresponding author. Fax: +91 2225724089.
E-mail address: mathur@chem.iitb.ac.in (P. Mathur).

0022-328X/$ - see front matter © 2006 Elsevier B.V. All rights reserved.
doi:10.1016/j.jorganchem.2006.04.016

were treated with $[Fe_3(CO)_9(\mu_3\text{-}S)_2]$ in the presence of different acetylenes HC≡CR (R = Ph), *n*-Bu or Fc$\{(\eta^5\text{-}C_5H_5)(\eta^5\text{-}C_5H_4)Fe\}$, we isolated mixed-metal clusters $[Fe_3M[(\eta^5\text{-}C_5Me_5)(CO)_6(\mu_3\text{-}S)(\mu_3\text{-}CCPh)\{\mu_3\text{-}C(H){=}C(R)S\}]$ (R = Ph, *n*-Bu and M = W, Mo) or $[Fe_3M[(\eta^5\text{-}C_5Me_5)\text{-}(CO)_7(\mu_3\text{-}S)(\mu_3\text{-}CCPh)\{\mu_3\text{-}C(Fc){=}C(H)S\}]$ (M = Mo, W), where a rare 'acetylide-flip' occurs with formation of {SC(H)CFc} ligand [8].

In this paper we report on our investigation of the reaction of iron pentacarbonyl and ferrocenylacetylene in the presence of S-powder and CS_2.

2. Results and discussion

2.1. Photolysis of solution containing $Fe(CO)_5$, ferrocenylacetylene and S-powder

When a mixture of $Fe(CO)_5$, ferrocenylacetylene and S-powder in hexane solvent was photolysed under constant bubbling of argon for 10 min at −30 °C, formation of new adducts $[\{\mu\text{-}SC(H){=}C(Fc)S\}(CO)_6Fe_2]$ (**1**) and $[\mu\text{-}SC(O)\text{-}C(H){=}C(Fc)S\}(CO)_6Fe_2]$ (**2**) was observed (Scheme 1). These were isolated by chromatographic work-up as air-stable crystalline solids.

The structural features of **1** and **2** were identified on the basis of IR and ^1H and ^{13}C NMR spectroscopy (Table 1). The IR spectra of **1** and **2** display carbonyl stretching patterns typically observed in the spectra of compounds containing the $Fe_2(CO)_6$ groups. The spectrum of compound **1** displays a carbonyl stretching pattern which is identical to that observed for earlier reported $[\{\mu\text{-}EC(H){=}C(R)E'\}\text{-}(CO)_6Fe_2]$ (E, E′ = S, Se,Te; R = Ph, Th, C≡CCH_3) [9–17]. Compound **2** shows a band due to the presence of a ketonic carbonyl group at 1655 cm^{-1}, in addition to the terminal carbonyl bands. The ^1H and ^{13}C NMR spectra confirm the presence of ferrocenyl, ethylenic, carbonyl and ketonic carbonyl groups. The ^1H NMR spectra of **1** and **2** each display four sets of signals: three signals for ferrocenyl ring protons and a signal for CH proton. Dark brown crystals of **1** and bluish green crystals of **2** were

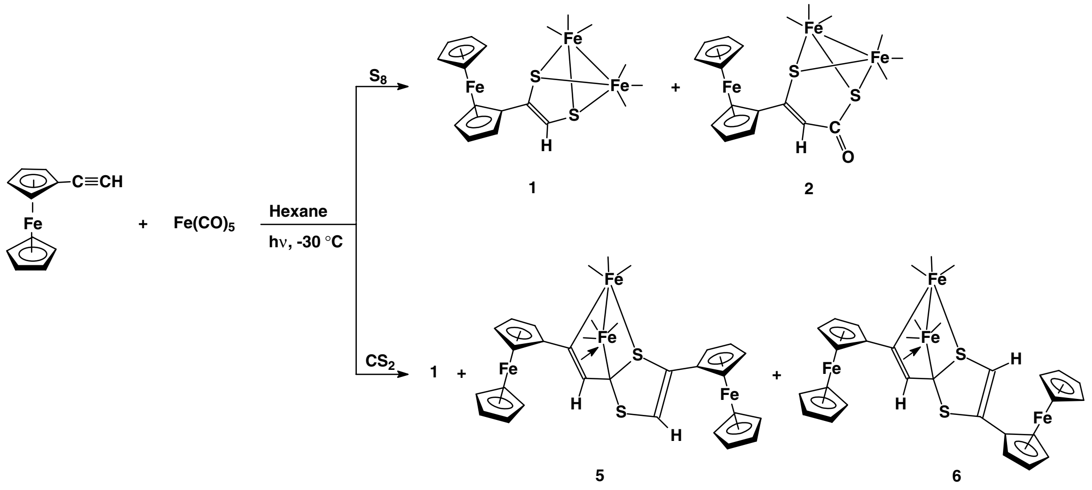

Scheme 1.

Table 1
Spectroscopic data for compounds **1**, **2**, **5** and **6**

Compound	IR [ν(CO), cm^{-1}, hexane]	^1H NMR (δ, $CDCl_3$)	^{13}C NMR (δ, $CDCl_3$)
1	2076 (s), 2040 (vs), 2003 (vs)	4.20 (s, 2H, sub Cp), 4.28 (s, 5H, unsub Cp), 4.32 (s, 2H, sub Cp), 5.94 (s, 1H, FcCC*H*)	67.3–77.7 (sub Cp carbons), 69.9 (unsub Cp carbons), 128.1 (*C*H), 134.3 (*C*CH), 208.1–217.1 (*C*O)
2	2080 (vs), 2046 (vs), 2009 (vs), 1655 (m)	4.30 (s, 5H, unsub Cp ring), 4.64 (s, 4H, sub Cp ring), 5.51 (s, 1H, FcC=C(*H*))	68.8–76.4 (sub Cp carbons), 71.2 (unsub Cp carbons), 125.9 (*C*H), 144.2 (*C*CH), 199.4 (*C*(O)CH), 206.5–219.3 (*C*O)
5	2062 (vs), 2020 (vs), 1999 (s)	4.12 (s, 5H, unsub Cp ring), 4.27 (s, 5H, unsub Cp ring), 4.31–4.75 (m, 8H, sub Cp rings), 6.24 (s, 1H, FcC=C(*H*)C–), 6.79 (s, 1H, FcCC(*H*)S–).	68.1–73.0 (sub Cp carbons), 70.2, 70.3 (unsub Cp carbons), 79. (*C*$CHCS_2$), 95.0 (*C*HCS_2), 123.0 (S*C*H), 146.1 (S*C*Fc), 173.8 (CS_2), 207.4–219.0 (*C*O)
6	2061 (s), 2019 (vs), 1996 (m)	4.25 (s, 5H, unsub Cp ring), 4.27 (s, 5H, unsub Cp ring), 4.35–4.75 (m, 8H, sub Cp rings), 5.97 (s, 1H, FcC=C(*H*)C–), 6.25 (s, 1H, FcCC(*H*)S–)	69.5–73.8 (sub Cp carbons), 70.2, 70.2 (unsub Cp carbons), 87.1 (*C*$CHCS_2$), 95.1 (*C*HCS_2), 121.1 (S*C*H), 155.5 (S*C*Fc), 169.7 (CS_2), 202.7–222.8 (*C*O)

grown from dichloromethane/hexane solvent mixtures at 0 °C and single crystal X-ray diffraction study was carried out to determine their molecular structures. ORTEP plots of molecular structure of **1** and **2**, along with selected bond metricals, are shown in Figs. 1 and 2, respectively.

Acetylenes ($RC{\equiv}CH$, R = H, Ph) are known to add across the chalcogen–chalcogen bonds of $[Fe_2(CO)_6(\mu\text{-}EE')]$ (for all combinations of E, E′ = S, Se, Te except E = E′ = S) to yield the adducts $[Fe_2(CO)_6\{\mu\text{-}EC(R){=}C(H)E'\}]$. The S_2 analog, $[Fe_2(CO)_6\{\mu\text{-}SC(H){=}C(H)S\}]$ has been obtained by reacting $HC{\equiv}CMgBr$ with $[Fe_2(CO)_6S_2]$, followed by protonation with CF_3CO_2H; and its identification is based on spectrometric characterisation. We attempted to prepare **1** by the method used for obtaining $[Fe_2(CO)_6\{\mu\text{-}EC(R){=}C(H)E'\}]$, of room temperature stirring of solution containing $[Fe_2(CO)_6S_2]$ with ferrocenylacetylene in presence of sodium acetate, but did not observe any formation of **1**. Irradiation with UV light of a hexane solution containing $[Fe_2(CO)_6S_2]$ and ferrocenylacetylene did not yield any **1**, or **2** when the photolysis was carried out in presence of CO.

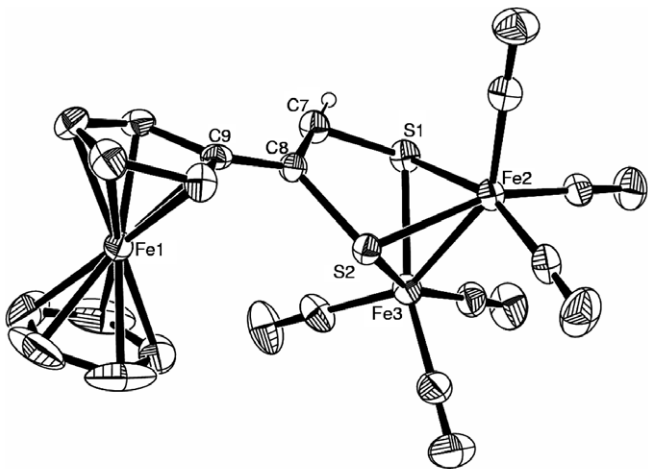

Fig. 1. ORTEP diagram of **1** with 50% probability ellipsoids. Selected bond distances (Å) and bond angles (°): Fe(2)–Fe(3) = 2.4755 (12), Fe(2)–S(1) = 2.2847(18), Fe(2)–S(2) = 2.2658(16), Fe(3)–S(1) = 2.273(2), Fe(3)–S(2) = 2.2754(17), C(7)–C(8) = 1.313 (8), C(8)–C(9) = 1.439(7), S(1)–C(7) = 1.805(6), S(2)–C(8) = 1.810(6); and C(7)–C(8)–C(9) = 128.3(6), S(1)–Fe(2)–S(2) = 79.45(6), S(1)–Fe(3)–S(2) = 79.49(6), C(8)–C(7)–S(1) = 117.3 (5), C(8)–S(2)–Fe(2) = 103.08(19), C(8)–S(2)–Fe(3) = 101.54(19), S(1)–Fe(3)–Fe(2) = 57.33(5).

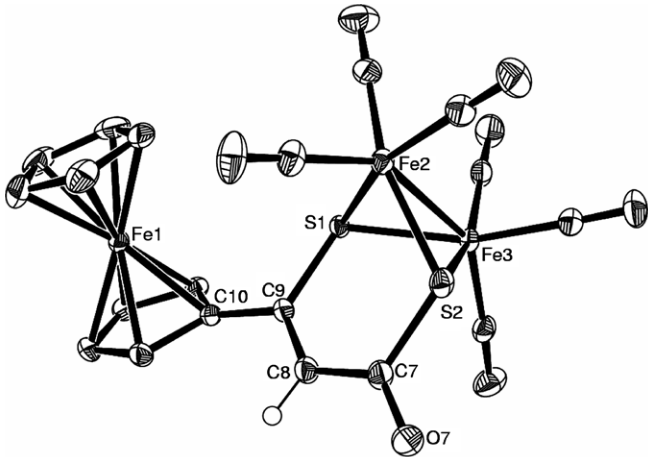

Fig. 2. ORTEP diagram of **2** with 50% probability ellipsoids. Selected bond distances (Å) and bond angles (°): Fe(2)–Fe(3) = 2.5077(3), Fe(2)–S(1) = 2.2594(4), Fe(2)–S(2) = 2.2564(5), Fe(3)–S(1) = 2.2642(4), Fe(3)–S(2) = 2.2648(5), C(7)–C(8) = 1.452(2), C(8)–C(9) = 1.348(2), C(9)–C(10) = 1.460(2), S(1)–C(9) = 1.7854(15), C(7)–O(7) = 1.213(2); and S(1)–Fe(2)–S(2) = 85.882(16), S(1)–Fe(3)–S(2) = 85.571(16), C(7)–C(8)–C(9) = 127.78(15), C(8)–C(9)–C(10) = 120.16(14), C(8)–C(9)–S(1) = 125.18(12), C(9)–S(1)–Fe(3) = 113.69(5), C(9)–S(1)–Fe(2) = 108.97(5), C(8)–C(7)–S(2) = 122.04(12), O(7)–C(7)–S(2) = 115.08(13), S(1)–Fe(2)–Fe(3) = 56.425(12).

Under photolytic conditions, it is possible that a partial decomposition of $Fe(CO)_5$ to form $Fe(CO)_x$ fragments influences the reactivity of ferrocenylacetylene towards the synthesis. Structures of **1** and **2** both feature a butterfly $Fe_2(CO)_6S_2$ unit; in **1** there is a $FcC{=}CH$ unit added across the open butterfly edge while in **2** a $FcC{=}C(H)(CO)$ adds to the S atoms to complete the structure. Overall, the structure of **1** is similar to $[\{\mu\text{-}SeC(H){=}C(Ph)E\}(CO)_6Fe_2]$ (E = S [9], Se [10], Te [11]), $[\{\mu\text{-}SC(H){=}C(Ph)Te\}(CO)_6Fe_2]$ [10], $[\{\mu\text{-}TeC(H){=}C(Ph)Te\}(CO)_6Fe_2]$ [12], $[\{\mu\text{-}SeC(H){=}C(2\text{-}Th)Se\}(CO)_6Fe_2]$ [13], and $[\{\mu\text{-}SC(C{\equiv}CCH_3){=}C(H)Te\}(CO)_6Fe_2]$ [14]. The C–C bond distance of 1.313(8) Å in **1** and 1.348(2) Å in **2** indicates the reduction of the acetylenic triple bond to an olefinic bond order and is similar to corresponding bond distances of the coordinated acetylenic bond in $[\{\mu\text{-}SeC(H){=}C(Ph)Se\}(CO)_6Fe_2]$ (1.331(7) Å), [10] $[\{\mu\text{-}SeC(H){=}C(Ph)S\}(CO)_6Fe_2]$ (1.293(13) Å) [9], $[\{\mu\text{-}SC(H){=}C(Ph)Te\}(CO)_6Fe_2]$ (1.32(1) Å) [9], $[\{\mu\text{-}SeC(H){=}C(Ph)Te\}(CO)_6Fe_2]$ (1.31(3) Å) [11], $[\{\mu\text{-}TeC(H){=}C(Ph)Te\}(CO)_6Fe_2]$ (1.34(1) Å) [12], $[\{\mu\text{-}SeC(H){=}C(2\text{-}Th)Se\}(CO)_6Fe_2]$ (1.306(14) Å) [13], $[\{\mu\text{-}SC(C{\equiv}CCH_3){=}C(H)Te\}(CO)_6Fe_2]$ (1.31(1) Å) [14]. The Fe–Fe bond distance of 2.4755(12) Å in **1** is the shortest among the compounds $[\{\mu\text{-}SC(O)C(H){=}C(Fc)S\}(CO)_6Fe_2]$ (2.5077(3) Å) in **2**, $[\{\mu\text{-}TeC(H){=}C(Ph)Te\}(CO)_6Fe_2]$ (2.571(4) Å), $[\{\mu\text{-}SeC(H){=}C(Ph)Te\}(CO)_6Fe_2]$ (2.539(5) Å), $[\{\mu\text{-}SC(H){=}C(Ph)Te\}(CO)_6Fe_2]$ (2.526(2) Å), $[\{\mu\text{-}SC(C{\equiv}CCH_3){=}C(H)Te\}(CO)_6Fe_2]$ (2.538(2) Å), $[\{\mu\text{-}SeC(H){=}C(Ph)S\}(CO)_6Fe_2]$ (2.501(3) Å), $[\{\mu\text{-}SeC(H){=}C(Ph)Se\}(CO)_6Fe_2]$ (2.512(1) Å), $[\{\mu\text{-}SeC(H){=}C(2\text{-}Th)Se\}(CO)_6Fe_2]$ (2.513(2) Å). The average Fe–S bond length of 2.2747 Å in **1** and 2.2612 Å in **2** is similar to the average Fe–S bond length of 2.289 Å in $[\{\mu\text{-}SeC(H){=}C(Ph)S\}(CO)_6Fe_2]$, 2.266 Å in $[\{\mu\text{-}SC(H){=}C(Ph)Te\}(CO)_6Fe_2]$ and 2.261 in $[\{\mu\text{-}SC(C{\equiv}CCH_3){=}C(H)Te\}(CO)_6Fe_2]$ but slightly longer than the corresponding average distance of 2.228 Å observed in $[(CO)_6Fe_2(\mu\text{-}S_2)]$. The average S–Fe–S bond angle of 79.49(6)° in **1** is marginally less than the 85.571(16)° in **2**. The angles are significantly greater than average S–Fe–S bond angle of 53.6° in $[(CO)_6Fe_2S_2]$, consistent with an almost equal amount of opening of the Fe_2S_2 butterfly cores to accommodate the different $RC{=}CH$ and $Fc{=}C(CO)H$ units into the open edges of the Fe_2EE' butterfly units.

Formation of **2**, which can formally be regarded as a CO insertion product of **1**, was not observed when a solution of

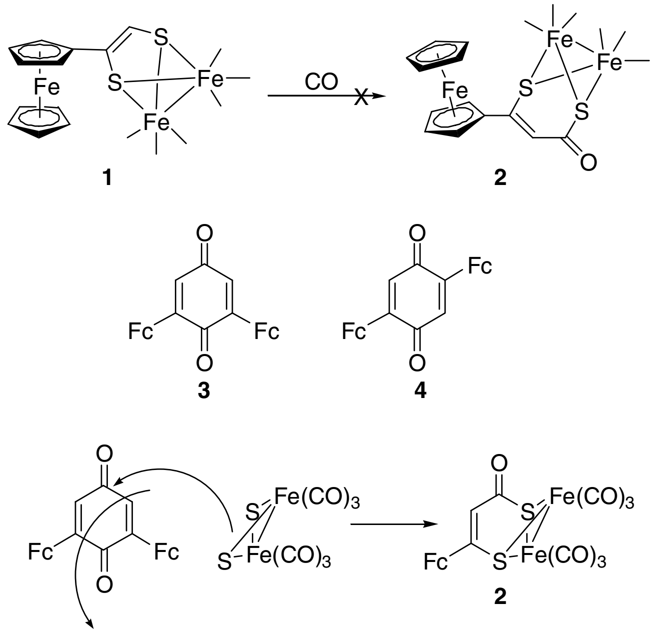

Scheme 2.

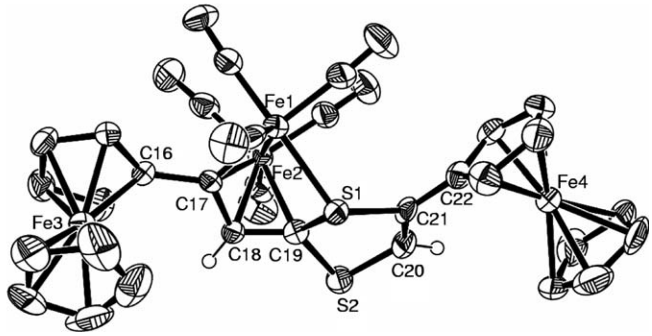

Fig. 3. ORTEP diagram of **5** with 50% probability ellipsoids. Selected bond distances (Å) and bond angles (°): Fe(1)–Fe(2) = 2.5957(15), C(16)–C(17) = 1.477(9), C(17)–C(18) = 1.418(9), C(18)–C(19) = 1.415(9), C(20)–C(21) = 1.319(10), C(21)–C(22) = 1.472(10), Fe(2)–C(17) = 2.093(7), Fe(2)–C(18) = 2.054(7), Fe(2)–C(19) = 2.064(8), Fe(1)–C(17) = 2.029(7), Fe(1)–S(1) = 2.282(2), S(1)–C(19) = 1.776(7), S(2)–C(19) = 1.782(8), S(2)–C(20) = 1.756(8), S(1)–C(21) = 1.785(6); and C(18)–C(17)–C(16) = 119.2(6), C(16)–C(17)–Fe(1) = 125.7(5), C(16)–C(17)–Fe(2) = 124.7(5), C(19)–C(18)–C(17) = 113.1(6), C(18)–C(19)–S(1) = 113.4(5), C(18)–C(19)–S(2) = 128.2(6), C(20)–C(21)–C(22) = 127.2(6), C(20)–C(21)–S(1) = 112.5(6), C(22)–C(21)–S(1) = 119.7(6), C(20)–S(2)–C(19) = 90.3(4), C(18)–Fe(2)–Fe(1) = 77.0(2), C(17)–Fe(1)–Fe(2) = 52.1(2), S(1)–C(19)–S(2) = 109.5(4), S(1)–Fe(1)–Fe(2) = 79.18(6).

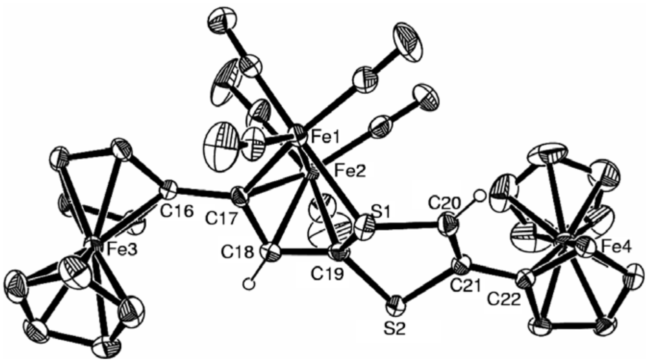

Fig. 4. ORTEP diagram of **6** with 50 % probability ellipsoids. Selected bond distances (Å) and bond angles (°): Fe(1)–Fe(2) = 2.5969(11), C(16)–C(17) = 1.485(6), C(17)–C(18) = 1.412(7), C(18)–C(19) = 1.422(7), C(20)–C(21) = 1.341(7), C(21)–C(22) = 1.466(7), Fe(2)–C(17) = 2.083(5), Fe(2)–C(18) = 2.057(5), Fe(2)–C(19) = 2.066(5), Fe(1)–C(17) = 2.015(5), Fe(1)–S(1) = 2.2793(17), S(1)–C(19) = 1.774(5), S(2)–C(19) = 1.779(5), S(1)–C(20) = 1.754(5), S(2)–C(21) = 1.775(5); and C(18)–C(17)–C(16) = 118.3(5), C(16)–C(17)–Fe(1) = 125.7(4), C(16)–C(17)–Fe(2) = 125.8(3), C(17)–C(18)–C(19) = 113.0(5), C(18)–C(19)–S(1) = 112.6(4), C(18)–C(19)–S(2) = 129.2(4), C(20)–C(21)–C(22) = 126.5(5), C(21)–C(20)–S(1) = 115.3(4), C(22)–C(21)–S(1) = 117.1(4), C(21)–S(2)–C(19) = 91.8(3), C(18)–Fe(2)–Fe(1) = 76.76(15), C(17)–Fe(1)–Fe(2) = 51.84(14), S(1)–C(19)–S(2) = 108.5(3), S(1)–Fe(1)–Fe(2) = 78.89(4).

1 was bubbled with CO (Scheme 2) under thermolytic or photolytic conditions.

In our attempt to obtain **2** from **1** and CO under photolytic conditions, we did observe trace amounts of the previously reported quinones, **3** and **4**, and though **2** can be regarded as resulting from a formal substitution of a {HC=C(Fc)C(O)} unit, by {$Fe_2S_2(CO)_6$}, we were unable to obtain **2** from the reaction of the quinones with [$Fe_2S_2(CO)_6$] or $Fe(CO)_5$/S under photolytic conditions (Scheme 2).

2.2. Photolysis of solution containing Fe(CO)$_5$, ferrocenylacetylene and CS$_2$

When a hexane solution containing $Fe(CO)_5$, ferrocenylacetylene and CS_2 was photolyzed under constant bubbling of argon for 10 min at −30 °C, formation of new compounds *cis*-[μ-η^1:η^2:η^1:η^1-{C(Fc)=C(H)CS$_2$C(H)=C(Fc)}(CO)$_6$Fe$_2$] (**5**) and *trans*-[μ-η^1:η^2:η^1:η^1-{C(Fc)=C(H)CS$_2$C(Fc)=C(H)}(CO)$_6$Fe$_2$] (**6**) were observed along with the adduct **1** (Scheme 1).

Compounds **5** and **6** were characterized by IR and ^{1}H and ^{13}C NMR spectroscopy (Table 1). These compounds are stable in solid state and in solution state over a period of days. The IR spectra of the two compounds show the presence of only terminal carbonyls and both compounds display an identical carbonyl stretching pattern characteristic of a $Fe_2(CO)_6$ group. ^{1}H and ^{13}C NMR spectra of **5** and **6** confirm the presence of C_2H unit, CS_2, ferrocenyl and carbonyl groups. Dark-red single crystals of **5** and **6** were grown from dichloromethane/hexane solvent mixtures at 0 °C, and their structures were established crystallographically. An ORTEP plot of molecular structure of **5** and **6**, along with selected bond metricals are shown in Figs. 3 and 4, respectively.

The formation of **5** and **6** involve the coupling of two ferrocenylacetylene molecules with CS_2 leading to the formation of 3,5-dithia-4-ethynylferrocenyl-1-ferrocenylcyclopentene ligand bonded to the $Fe_2(CO)_6$ group in a η^1:η^2:η^1:η^1 fashion. This contrasts with the earlier reported CS_2 insertions into metal–acetylene bonds; in the reaction of [(L)Mo(CO)$_3$(C≡CPh)] L = (η^5-C_5H_5)

and (η^5-C_5Me_5), with CS_2, both η^2- and η^3-coordinated CS_2 bonding modes were observed to give $S_2CC{\equiv}CPh$ ligand system [18]. Each Fe atom has three terminally bonded carbonyl groups. The two ferrocenyl groups are mutually *cis*-(**5**) and *trans*-(**6**) oriented. Delocalization of π-electron cloud over FcC–C–CS_2 in **5** and **6** is indicated by shortening of C(18)–C(19) single bond to 1.415(9) in **5** and 1.422(7) in **6** and lengthening of C(17)–C(18) bond to 1.418(9) in **5** and 1.412(7) Å in **6** from the normal values associated with C–C single bond (1.5 Å) and C≡C triple bonds (1.1 Å), respectively.

To satisfy electron counting at Fe(2) atom, we believe that there must exist a π-bond between the C(Fc)=CCS_2 and the iron centre. Indeed, the C(olefin)–Fe distances in **5** and **6** (average C(17)–Fe(2), 2.088 Å and average C(18)–Fe(2), 2.0555 Å) compare well with the average distances observed between the coordinated olefinic carbons and the iron atom in $[Fe(\eta^5\text{-}C_5H_4E^ICH_2C{\equiv}CH)\eta^5\text{-}C_5\text{-}H_4\{Fe_2M(CO)_8(\mu\text{-}E)(\mu_3\text{-}E)(E^ICHCCH_2)\}]$ (M = Fe, E^I = Se, E = Se; M = Fe, E^I = Se, E = S; M = Ru, E^I = Se, E = S) (average C(14)–Fe(2) = 2.042 Å and average C(15)–Fe(2) = 2.051 Å) [19], in $[Fe(CO)_4(\eta^2\text{-}CH_2CHCN)]$ (2.10 Å) [20], $[Fe(CO)_4(\eta^2\text{-}C_6H_8)]$ (2.15 Å) [21] and in $[Fe(CO)_3(\eta^2C_6H_4(CH{=}CH_2)(PPh_2))]$ (2.05 Å) [22]. However, the C(Fc)=CCS_2 bond distances of 1.418(9) Å in **5** and 1.412(7) Å in **6** are somewhat longer than the C=C bond distance of 1.35–1.39 Å in $[Fe(\eta^5C_5H_4E^ICH_2C{\equiv}CH)\eta^5\text{-}C_5H_4\{Fe_2M(CO)_8\text{-}(\mu\text{-}E)(\mu_3\text{-}E)(E^ICHCC\text{-}H_2)\}]$, but comparable with the C=C bond distances reported in other iron-olefin complexes, $[Fe(CO)_4(\eta^2\text{-}CH_2CHCN)]$, 1.40(2) Å, $[Fe(CO)_4(\eta^2\text{-}C_6H_8)]$, 1.421(5) Å and $[Fe(CO)_3(\eta^2C_6H_4(CH{=}CH_2)(PPh_2))]$, 1.45 Å. The C(20)–C(21) bond distance of 1.319(2) Å in **5** and 1.341(7) Å in **6** indicates the reduction of the acetylenic triple bond to an olefinic bond order. It is similar to corresponding bond distances of the coordinated acetylenic bond in $[\{\mu\text{-}SeC(H){=}C(Ph)Se\}(CO)_6Fe_2]$ (1.331(7) Å), $[\{\mu TeC(H){=}C(Ph)Te\}(CO)_6Fe_2]$ (1.34(1) Å). The Fe–Fe bond distance of 2.5957(15) Å in **5** and 2.5969(11) Å in **6** is comparable with the corresponding distances in $\{\mu TeC(H){=}C(Ph)Te\}(CO)_6Fe_2]$(2.571(4) Å) and in $[\{\mu\text{-}SeC(H){=}C(Ph)\text{-}Te\}(CO)_6Fe_2]$ (2.539(5) Å) but somewhat longer than the corresponding distances observed in the compounds **1** (2.4755(12) Å) and **2** (2.5077(3) Å) reported herein and in $[\{\mu\text{-}SeC(H){=}C(Ph)S\}(CO)_6Fe_2]$ (2.501(3) Å). The Fe(1)–S(1) bond distance of 2.282(2) Å in **5** and 2.279(17) Å in **6** is comparable with the average Fe–S bond distances of 2.2893 Å in $[\{\mu\text{-}SeC(H){=}C(Ph)S\}(CO)_6Fe_2]$, 2.263(2) Å in $[\{\mu SC(H){=}C(Ph)Te\}(CO)_6Fe_2]$ and 2.261 Å in $[\{\mu\text{-}SC(C{\equiv}CCH_3){=}C(H)Te\}(CO)_6Fe_2]$ but longer than the average Fe–S bond distances of 2.228 Å observed in $(CO)_6Fe_2S_2$. The average C–S bond distances of 1.77475 Å in **5** and 1.7705 Å in **6** is comparable with 1.763(3) Å in $[(\eta^5\text{-}C_5Me_5)MoFe_3(\mu_3\text{-}S)\{(\mu_3\text{-}C(H){=}C(Ph)S\}(CO)_6(\mu_3\text{-}CCPh)]$ [8], but slightly shorter than the C–S bond distance in $Os_4(CO)_{12}[\mu_4\text{-}\eta^3\text{-}SC(Ph){=}CH]$ (1.817(11) Å) [23]. The S–C–S bond angle of 109.5(4)° in **5** and 108.5(3)° in **6** is similar to the S–C–S bond angle of 110.6(2)° in $[(\eta^5\text{-}C_5H_5)Mo(CO)_2(\eta^2\text{-}S_2CC{\equiv}CPh)]$, and 108.6(6)° in $[(\eta^5\text{-}C_5Me_5)Mo(CO)_2CS_2)\{W(CO)_5\}_2C{\equiv}CPh]$ [18].

3. Conclusion

Although the formation of **1** and **2** appear to be straightforward addition of FcC≡CH and FcC=C(H)C(O) units respectively to $Fe_2(CO)_6S_2$ units they could not be obtained by direct reaction of FcC≡CH with $[Fe_2(CO)_6S_2]$ in absence or presence of CO. The exact mechanism of formation of **1** and **2** cannot be ascertained at this time, however, it is possible to propose one involving an initial formation of $Fe(CO)_x$ or $Fe_2(CO)_y$ fragments, under the photolytic conditions used, followed by coordination of ferrocenylacetylene to the coordinatively unsaturated fragments and insertion of S, and of CO (in case of **2**) to give the final products. In the case of **5** and **6**, the formal insertion of CS_2 facilitates two ferrocenylacetylenes to add on and form the unusual ligand system, $FcC{=}C(H)CS_2C(H){=}CFc$, arising from coupling of two ferrocenylacetylenes with a CS_2 molecule on a $Fe_2(CO)_6$ unit.

4. Experimental

4.1. General procedure

Reactions and manipulations were performed using standard Schlenk techniques under an atmosphere of prepurified argon. Solvents were purified, dried and distilled under an argon atmosphere prior to use. Infrared spectra were recorded on a Nicolet Impact 400 FT spectrometer as hexane solutions in 0.1 mm path length NaCl cells and NMR spectra on a Varian VXRO-300S spectrometer in $CDCl_3$. Elemental analyses were performed on a Carlo-Erba automatic analyzer. The compound FcC≡CH was prepared as reported earlier [24]. Iron pentacarbonyl, ferrocene, S-and Se-powder were purchased from Fluka, Spectrochem and s.d. fine-chem Ltd., respectively and these were used without further purification. TLC plates were purchased from Merck (20 × 20 cm, Silica gel 60 F_{254}). Photochemical reactions were carried out using double-walled quartz vessel having a 125 W immersion type mercury lamp manufactured by Applied Photophysics Ltd.

4.2. Preparation of $(CO)_6Fe_2\{\mu\text{-}SC(H){=}C(Fc)S\}$ (1) and $(CO)_6Fe_2\{\mu\text{-}SC(O)C(H){=}C(Fc)S\}$ (2)

A hexane solution (50 mL) containing $Fe(CO)_5$ (98 mg, 0.5 mmol), FcC≡CH (105 mg, 0.5 mmol) and S-powder (32 mg, 1.0 mmol) was subjected to photolysis for 10 min at −30 °C in a photochemical reaction vessel under a continuous argon flow. The solvent was removed in vacuo and the residue was dissolved in dichloromethane. The dichloromethane solution was filtered through Celite to remove insoluble materials. The solution was subjected to chromatographic work-up using silica-gel TLC plates. Elution with hexane yielded a brown band of $[(CO)_6Fe_2\{\mu\text{-}SC(H){=}C(Fc)S\}]$ (**1**), and a yellow $FcC{\equiv}CH$. Further elution with dichloromethane/hexane (20:80 v/v) mixture yielded a blue-green band of $(CO)_6Fe_2\{\mu\text{-}SC(O)C(H){=}C(Fc)S\}$ (**2**). Reaction of $Fe(CO)_5$, $FcC{\equiv}CH$ and Se-powder gave a number of bands and all of them were of insufficient amount to facilitate their isolation and characterization.

4.3. Preparation of $[(CO)_6Fe_2\{\mu\text{-}SC(H){=}C(Fc)S\}]$ (1), cis-$[\mu\text{-}\eta^1{:}\eta^2{:}\eta^1{:}\eta^1\text{-}\{C(Fc){=}C(H)CS_2C(H){=}C(Fc)\}\text{-}(CO)_6Fe_2]$ (5) and trans-$[\mu\text{-}\eta^1{:}\eta^2{:}\eta^1{:}\eta^1\text{-}\{C(Fc){=}C(H)\text{-}CS_2C(Fc){=}C(H)\}(CO)_6Fe_2]$ (6)

A hexane solution (50 mL) containing $Fe(CO)_5$ (98 mg, 0.5 mmol), $FcC{\equiv}CH$ (105 mg, 0.5 mmol) and CS_2 (76 mg, 1.0 mmol) was subjected to photolysis for

Table 2
Experimental conditions used for the preparation of **1**, **2**, **5** and **6**

$Fe(CO)_5$ [mg (mmol) (used)]	$[(\eta^5\text{-}C_5H_5)Fe(\eta^5\text{-}C_5H_4C{\equiv}CH)]$ [mg (mmol)] [mg (mmol) (recovered)]	L [mg (mmol) (used)]	Product obtained	Yield[a]: Mg (%)	Anal. Calc. (found)	MP/°C
[98 (0.5)]	[105 (0.5)] [54 (0.26)]	S [32 (1.0)]	**1**	18 (13)	C, 38.99 (38.78) H, 1.80 (1.90) S, 11.55 (11.42)	205–207[b]
		–	**2**	24 (17)	C, 39.18 (39.32) H, 1.72 (1.77) S, 11.00 (10.76)	246–248[b]
[98 (0.5)]	[105 (0.5)] [38 (0.18)]	CS_2 [76 (1.0)]	**1**	28 (16)	–	–
			5	19 (15)	C, 47.94 (47.67) H, 2.58 (2.30) S, 8.25 (8.01)	185–187[b]
			6	24 (19)	C, 47.94 (47.81) H, 2.58 (2.39) S, 8.25 (8.09)	196–199[b]

[a] Based on amount of $[(\eta^5\text{-}C_5H_5)Fe(\eta^5\text{-}C_5H_4C{\equiv}CH)]$ consumed.
[b] Decomposed.

Table 3
Crystal data and structure refinement parameters for **1**, **2**, **5** and **6**

	1	**2**	**5**	**6**
Formula	$C_{18}H_{10}Fe_3O_6S_2$	$C_{19}H_{10}Fe_3O_7S_2$	$C_{31}H_{20}Fe_4O_6S_2$	$C_{31}H_{20}Fe_4O_6S_2$
Molecular weight	553.93	581.94	775.99	775.99
Temperature (K)	293(2)	133(2)	293(2)	293(2)
Crystal system	Monoclinic	Monoclinic	Orthorhombic	Monoclinic
Space group	$P2_1/c$	$P2_1/c$	$P2_12_12_1$	$C2/c$
a (Å)	7.6390(10)	12.7115(8)	7.5030(10)	37.3320(14)
b (Å)	10.4380(5)	7.4774(4)	12.4990(9)	7.6610(7)
c (Å)	25.5310(17)	21.3879(14)	31.2060(15)	21.6950(10)
α (°)	90	90	90	90
β (°)	97.607(7)	90.222(3)	90	106.324(4)
γ (°)	90	90	90	90
V (Å^3)	1493.3(3)	2032.9(2)	2926.5(5)	5954.6(6)
Z	4	4	4	8
D_{calc} (Mg/m^{-3})	1.823	1.901	1.761	1.731
Absorption coefficient (mm^{-1})	2.367	2.358	2.131	2.094
$F(000)$	1104	1160	1560	3120
Crystal size (mm)	0.40 × 0.13 × 0.08	0.44 × 0.41 × 0.15	0.30 × 0.13 × 0.10	0.40 × 0.15 × 0.15
θ Range (°)	1.61–24.98	1.60–30.03	1.30–24.94	1.96–25.00
Index ranges	$0 \leqslant h \leqslant 9$, $-12 \leqslant k \leqslant 0$, $-30 \leqslant l \leqslant 30$	$-17 \leqslant h \leqslant 17$, $-10 \leqslant k \leqslant 10$, $-30 \leqslant l \leqslant 30$	$-8 \leqslant h \leqslant 0$, $0 \leqslant k \leqslant 14$, $0 \leqslant l \leqslant 37$	$0 \leqslant h \leqslant 44$, $-9 \leqslant k \leqslant 0$, $-25 \leqslant l \leqslant 24$
Number of reflections collected/unique [R_{int}]	3826/3541 [0.0304]	5949 [0.0297]	2927/2927 [0.0000]	5302/5215 [0.0265]
Number of data/restraints/parameters	3541/0/263	5949/0/280	2927/0/388	5215/0/388
Goodness-of-fit on F^2	1.020	1.071	1.018	1.008
Final R indices [$I > 2\sigma(I)$]	$R_1 = 0.0467$ $wR_2 = 0.1037$	$R_1 = 0.0232$ $wR_2 = 0.0564$	$R_1 = 0.0367$ $wR_2 = 0.0728$	$R_1 = 0.0484$ $wR_2 = 0.1068$
R indices (all data)	$R_1 = 0.1261$ $wR_2 = 0.1279$	$R_1 = 0.0332$ $wR_2 = 0.0615$	$R_1 = 0.0869$ $wR_2 = 0.0837$	$R_1 = 0.1085$ $wR_2 = 0.1242$
Largest difference in peak and hole (e Å^{-3})	0.611 and −0.529	0.566 and −0.315	0.428 and −0.476	0.639 and −0.734

10 min at −30 °C in a photochemical reaction vessel under a continuous argon flow. The solvent was removed in vacuo and the residue was dissolved in dichloromethane. The dichloromethane solution was filtered through Celite to remove insoluble materials. The solution was subjected to chromatographic work-up using silica-gel TLC plates. Elution with hexane yielded a brown band of [(CO)$_6$Fe$_2${μ-SC(H)=C(Fc)S}] (**1**), and a yellow FcC CH. Further elution with acetone/hexane (2:98 v/v) mixture yielded a red band of *trans*-[μ-η^1:η^2:η^1:η^1-{C(Fc)=C(H)CS$_2$C(H)=C(Fc)}(CO)$_6$Fe$_2$] (**6**); and a red *cis*-[μ-η^1:η^2:η^1:η^1-{C(Fc)=C(H)CS$_2$C(Fc)=C(H)}(CO)$_6$Fe$_2$] (**5**). Some other bands were also observed but these were of insufficient amounts to facilitate their isolation and characterization.

Details of the quantities of starting materials used, micro-analytical data, melting points and yields of the products are listed in Table 2.

4.4. Crystal structure determination of 1–5

Suitable X-ray quality crystals of **1**, **2**, **5** and **6** were grown by slow evaporation of dichloromethane/*n*-hexane solvent mixture at 0 °C, and an X-ray crystallographic data were recorded from single-crystal samples of **1** $(0.40 \times 0.13 \times 0.08)$ mm^3, **2** $(0.44 \times 0.41 \times 0.15)$ mm^3, **5** $(0.30 \times 0.13 \times 0.10)$ mm^3 and $(0.40 \times 0.15 \times 0.15)$ mm^3 **6**, mounted on glass fibers. Relevant crystallographic data and structure refinement details are listed in Table 3. Bruker Smart 1000CCD area detector diffractometer equipped with an LT-2 low-temperature attachment was used for the cell determination and intensity data collection for compound **2**. For crystals of **1**, **5** and **6**, a Nonius MACH3 diffractometer was used for cell determination and intensity data collection. Monochromated Mo Kα radiation ($\lambda = 0.71073$ Å) was used for the measurements. The unit cell parameters for **1**, **5** and **6** were derived and refined by using randomly selected reflections in the θ range 1.61–24.98° (**1**), 1.30–24.94° (**5**) and 1.96–25.00° (**6**). Appropriate empirical absorption corrections using the programs SADABS (for **2**) or ψ-scan (for **1**, **5** and **6**) were applied. The structures were solved by direct methods (SHELXS) and refined by full-matrix least-squares against F^2 using. SHELXL-97 (SHELX-TL for **2**) software [25]. Non-hydrogen atoms were refined with anisotropic thermal parameters. All hydrogen atoms were geometrically fixed and allowed to refine a riding model.

Crystallographic data (excluding structure factors) for the structures included in this paper have been deposited with the Cambridge Crystallographic Data Centre as supplementary Publication Nos. CCDC 287416 (**1**), CCDC 287419 (**2**), CCDC 287417 (**5**) and CCDC 287418 (**6**). These data can be obtained free of charge from The Cambridge Crystallographic Data Centre via www.ccdc.cam.ac.uk/data_request/cif.

Acknowledgements

P.M. is grateful to the Department of Science and Technology, Government of India for a research grant. V.K.S. and A.K.S. gratefully acknowledge the Council of Scientific and Industrial Research, Government of India for research fellowships.

Appendix A. Supplementary data

Supplementary data associated with this article can be found, in the online version, at doi:10.1016/j.jorganchem.2006.04.016.

References

[1] A.J.L. Pombeiro, R.L. Richards, Coord. Chem. Rev. 104 (1990) 13–38.
[2] T.J. Katz, S.M. Hacker, R.D. Kendrick, C.S. Yannoni, J. Am. Chem. Soc. 107 (1985) 2182–2183.
[3] (a) A.J. Deeming, Adv. Organomet. Chem. 26 (1986) 1–96;
(b) M.D. Vargas, J.N. Nicholls, Adv. Inorg. Chem. Radiochem. 30 (1986) 123–222;
(c) H. Bönnemann, Angew. Chem. 24 (1985) 248–262;
(d) E. Sappa, A. Tiripicchio, P. Braunstein, Chem. Rev. 83 (1983) 203–239.
[4] C.-W. Shiu, Y. Chi, C. Chung, S.-M. Peng, G.-H. Lee, Organometallics 17 (1998) 2970–2976.
[5] M. Akita, M. Terada, Y. Moro-oka, Chem. Commun. (1997) 265–266.
[6] (a) E. Sappa, J. Cluster Sci. 5 (1994) 211–263;
(b) A. Sironi, G. Gervasio, E. Sappa, J. Cluster Sci. 5 (1994) 535–549.
[7] P. Mathur, A.K. Bhunia, S.M. Mobin, V.K. Singh, Ch. Srinivasu, Organometallics 23 (2004) 3694–3700.
[8] P. Mathur, A.K. Bhunia, Ch. Srinivasu, S.M. Mobin, J. Organomet. Chem. 670 (2003) 144–150.
[9] P. Mathur, A.K. Dash, Md.M. Hossain, S.B. Umbarkar, C.V.V. Satyanarayana, Y.-S. Chen, E.M. Holt, S.N. Rao, M. Soriano, Organometallics 15 (1996) 1356–1361.
[10] P. Mathur, Md.M. Hossain, Organometallics 12 (1993) 2398–2400.
[11] P. Mathur, Md.M. Hossain, S.B. Umbarkar, C.V.V. Satyanarayana, S.S. Tavale, V.G. Puranik, Organometallics 14 (1995) 959–963.
[12] T. Fassler, D. Buchholz, G. Huttner, L. Zsolnai, J. Organomet. Chem. 369 (1989) 297–308.
[13] P. Mathur, A.K. Dash, Md.M. Hossain, C.V.V. Satyanarayana, A.L. Rheingold, G.P.A. Yap, L.M.L. Sands, J. Organomet. Chem. 543 (1997) 135–143.
[14] P. Mathur, Md.M. Hossain, S.N. Datta, R.-K. Kondru, M.M. Bhadbhade, Organometallics 13 (1994) 2532–2535.
[15] D. Seyferth, G.B. Womack, Organometallics 5 (1986) 2360–2370.
[16] C.W. Bird, E.M. Hollins, J. Organomet. Chem. 4 (1965) 245–246.
[17] G.N. Schrauzer, V.P. Mayweg, H.W. Fink, W. Heinrich, J. Am. Chem. Soc. 88 (1966) 4604–4609.
[18] P. Mathur, A.K. Ghosh, S. Mukhopadhyay, Ch. Srinivasu, S.M. Mobin, J. Organomet. Chem. 678 (2003) 142–147.
[19] P. Mathur, V.K. Singh, S.M. Mobin, Ch. Srinivasu, R. Trivedi, A.K. Bhunia, V.G. Puranik, Organometallics 24 (2005) 367–372.
[20] A.R. Luxmoore, M.R. Truter, Acta Crystallogr. 15 (1962) 1117–1124.
[21] F.A. Cotton, P. Lahuerta, Inorg. Chem. 14 (1975) 116–119.
[22] M.A. Bennett, G.B. Robertson, I.B. Tomkins, P.O. Whimp, J. Chem. Soc. Chem. Commun. (1971) 341–342.
[23] R.D. Adams, S. Wang, Organometallics 4 (1985) 1902–1903.
[24] G. Doisneau, G. Balavonie, T.F. Khan, J. Organomet. Chem. 425 (1992) 113–117.
[25] G.M. Sheldrick, SHELX 97. A Program for the Refinement of Crystal Structures, University of Göttingen, Göttingen, 1997.